



FTY720 Blocks Egress of T Cells in Part by Abrogation of Their Adhesion on the Lymph Node Sinus

This information is current as of September 2, 2011

Liang Zhi, Pilhan Kim, Brian D. Thompson, Costas Pitsillides, Alexander J. Bankovich, Seok-Hyun Yun, Charles P. Lin, Jason G. Cyster and Mei X. Wu

J Immunol 2011;187:2244-2251; Prepublished online 25 July 2011;

doi:10.4049/jimmunol.1100670

<http://www.jimmunol.org/content/187/5/2244>

-
- Supplementary Data** <http://www.jimmunol.org/content/suppl/2011/07/25/jimmunol.1100670.DC1.html>
- References** This article **cites 35 articles**, 16 of which can be accessed free at: <http://www.jimmunol.org/content/187/5/2244.full.html#ref-list-1>
- Subscriptions** Information about subscribing to *The Journal of Immunology* is online at <http://www.jimmunol.org/subscriptions>
- Permissions** Submit copyright permission requests at <http://www.aai.org/ji/copyright.html>
- Email Alerts** Receive free email-alerts when new articles cite this article. Sign up at <http://www.jimmunol.org/etoc/subscriptions.shtml/>



FTY720 Blocks Egress of T Cells in Part by Abrogation of Their Adhesion on the Lymph Node Sinus

Liang Zhi,^{*,†,1} Pilhan Kim,^{*,†,1,2} Brian D. Thompson,^{*,†} Costas Pitsillides,^{*,†} Alexander J. Bankovich,^{‡,§} Seok-Hyun Yun,^{*,†} Charles P. Lin,^{*,†} Jason G. Cyster,^{‡,§} and Mei X. Wu^{*,†}

Egress of lymphocytes from lymphoid tissues is a complex process in which G α i-mediated signals play a decisive role. We show here that although FTY720, an agonist of the sphingosine 1-phosphate (S1P)₁ receptor, induces S1P₁ receptor internalization sufficiently in the presence or absence of G α i2 or G α i3, the drug blocks egress of wild-type (WT) and G α i3-deficient T cells, but not G α i2-deficient T cells, in both WT and G α i2-deficient hosts. Intravital imaging of lymph nodes revealed that all three groups of T cells approached and engaged cortical sinusoids similarly in the presence or absence of FTY720. The cells also entered and departed the sinus at an almost identical frequency in the absence of the drug. However, after engagement of the sinus, most WT and G α i3-deficient T cells retracted and migrated back into the parenchyma in FTY720-treated animals, due to a failure of the cells to establish adhesion on the sinus, whereas G α i2-deficient T cells adhered firmly on the sinus, which prevented their retraction, facilitating their transmigration of the lymphatic endothelial barrier. These data confirm egress of G α i2^{-/-} T cells independent of S1P-mediated chemotaxis and failure of FTY720 to close lymphatic stromal channels and argue for the first time, to our knowledge, that FTY720 induces lymphopenia in part by impairing T cell adhesion to the sinus in a manner dependent on G α i2. *The Journal of Immunology*, 2011, 187: 2244–2251.

Sphingosine 1-phosphate (S1P) analogue FTY720 was approved recently by the U.S. Food and Drug Administration as a first-line treatment for relapsing forms of multiple sclerosis (1). It suppresses immune responses by blocking lymphocyte egress, but the underlying mechanism is not completely understood (2, 3). Early studies suggested that binding of FTY720 to the S1P₁ receptor (S1P₁R) caused internalization of the receptor in lymph node lymphocytes and thus prevented them from responding to a high concentration of S1P in the lymphatic sinus (4–7). This receptor internalization-dependent mechanism has been challenged by several investigations (8, 9). Sinha et al. (8) reported that egress of B lymphocytes from lymph nodes was not solely dependent on S1P-mediated chemotaxis (8). Also, pertussis toxin (PTX)-treated, S1P₁R-deficient T cells could exit lymph nodes, albeit at a reduced frequency (9). Moreover, in comparison with CCR7-positive T cells, CCR7-deficient T cells displayed

a compromised response to FTY720-induced lymphopenia (9). These investigations argue that a receptor internalization-independent mechanism, either alone or in conjunction with receptor internalization, is involved in FTY720-mediated blockade on lymphocyte egress.

S1P₁R is a G protein-coupled receptor and activates exclusively PTX-sensitive G α i/o proteins to propagate the entirety of its signal (10). The primary PTX substrates in T lymphocytes are G α i2 and G α i3 as shown by in vitro PTX labeling and cDNA cloning (11, 12). Our previous study has demonstrated that these two G α i proteins can be functionally overlapping, distinct, or antagonistic in chemotactic responses in a receptor-specific fashion (13, 14). In the current study, we use G α i2- and G α i3-deficient T cells, in conjunction with intravital time-lapse imaging, to delineate potentially distinct activities of these two G α i proteins in the multistep process of T cell egress. We find that in marked contrast to wild-type (WT) and G α i3-deficient T cells, G α i2-deficient T cells cannot be sequestered sufficiently in lymphoid tissue by FTY720. The drug appeared to diminish interactions between T cells and the sinus in the presence of G α i2 and to promote them migrating away from an exit, causing lymphopenia. The study suggests for the first time, to our knowledge, involvement of T cell adhesion to the sinus for T cell egress.

Materials and Methods

Mice

G α i2^{-/-}, G α i3^{-/-}, and WT control mice on a mixed 129Sv/C57BL/6 background were generous gifts from Dr. Lutz Birnbaumer (National Institute of Environmental Health Sciences, Research Triangle Park, NC) (15), and the mice were backcrossed with C57BL/6 mice six times as described (16). Both female and male mice were used at 4–6 wk of age unless otherwise indicated. The mice were housed in specific pathogen-free cages at the animal facilities of the Massachusetts General Hospital in accordance with institutional guidelines. The study was reviewed and approved by the Massachusetts General Hospital Subcommittee on Research Animal Care.

*Wellman Center for Photomedicine, Massachusetts General Hospital, Boston, MA 02114; [†]Department of Dermatology, Harvard Medical School, Boston, MA 02114; [‡]Howard Hughes Medical Institute, University of California at San Francisco, San Francisco, CA 94143; and [§]Department of Microbiology and Immunology, University of California at San Francisco, San Francisco, CA 94143

¹L.Z. and P.K. contributed equally to this work.

²Current address: Graduate School of Nanoscience and Technology, Korea Advanced Institute of Science and Technology, South Korea.

Received for publication March 7, 2011. Accepted for publication June 18, 2011.

This work was supported by National Institutes of Health Grants AI050822 and AI070785 and a Senior Research award from the Crohn's & Colitis Foundation of America (to M.X.W.).

Address correspondence and reprint requests to Dr. Mei X. Wu, Wellman Center of Photomedicine, Massachusetts General Hospital, 55 Fruit Street, Edwards 222, Boston, MA 02114. E-mail address: mwu2@partners.org

The online version of this article contains supplemental material.

Abbreviations used in this article: PTX, pertussis toxin; S1P, sphingosine 1-phosphate; S1P₁R, S1P₁ receptor; WT, wild-type.

Copyright © 2011 by The American Association of Immunologists, Inc. 0022-1767/11/\$16.00

In vivo flow cytometry

T cells were isolated from lymph nodes of the indicated mice as described previously (17), suspended in RPMI 1640 medium supplemented with 2% FBS, and stained with 10 μ M DiD (Invitrogen) for 30 min in a humidified incubator at 37°C followed by two washes with serum-free RPMI 1640. A total of 5×10^6 resultant cells per mouse were adoptively transferred into naive WT, $G\alpha i2^{-/-}$, or $G\alpha i3^{-/-}$ mice via the tail vein. The recipients were anesthetized 16 h later by i.p. injection of a mixture of ketamine (80 mg/kg) and xylazine (20 mg/kg). Fluorescently labeled donor cells were then counted by in vivo flow cytometry to establish control values before gavage of mice with either 1 mg/kg of FTY720 or 10 mg/kg of SEW2871 (Cayman Chemical). SEW2871 was administered every 12 h to maintain a sufficient level of the drug in the plasma (18). Fluorescently labeled cells in circulation were counted by in vivo flow cytometry at the indicated time points under anesthesia. The mouse to be examined by in vivo flow cytometry was positioned on a custom-built inverted microscope stage equipped with a warming tube to keep body temperature constant as described (19). A stationary laser beam was focused through cylindrical optics onto the ear blood vessel, forming a ~ 5 - μ m-wide slit whose long axis was perpendicular to the vessel, and the length was adjusted to match its diameter. As individual fluorescently labeled cells passed through the excitation beam, a burst of fluorescence was generated with a light-emitting diode at a wavelength of 633 nm, collected by the microscope objective lens, and detected by a photomultiplier tube through a confocal slit aperture. Matlab software developed in-house was used to determine the number of peaks per unit time as well as peak height and pulse width.

Infection of $G\alpha i2^{-/-}$ T cells with $G\alpha i2/3$ -expressing lentivirus

To generate a lentivirus expressing $G\alpha i2$ or $G\alpha i3$, $G\alpha i2$ or $G\alpha i3$ cDNA was subcloned into the multiple cloning site of a HIV-based lentiviral vector, pCDH1-copGFP (System Biosciences). The constructed and control GFP lentivirus were produced by transfection of the constructs individually into 293TN cells along with a ViralPower lentiviral packaging mix (System Biosciences). The culture supernatant was collected 48 h later, and viral titers were determined in 293TN cells based on the number of GFP⁺ cells at the highest titration of the supernatant. For infection, T cells prepared from $G\alpha i2^{-/-}$ mice were first stimulated with anti-CD3/anti-CD28 for 24 h to enhance their susceptibility to viral infection. Lentiviral culture supernatant was then added to the T cell culture at a virus to cell ratio of 20:1 to 50:1 overnight in the presence of 8 μ g/ml polybrene followed by culturing these cells for an additional 48 h after replenishment of half of the medium. The percentage of GFP⁺ cells was $\sim 35\%$ on average as determined by flow cytometry. The infected cells were administered i.v. into cognate WT mice at 4×10^6 cells per mouse. GFP⁺ cells were counted by in vivo flow cytometry before and after FTY720 treatment as above.

Intravital imaging and analysis of T cell egress

T cells isolated from WT, $G\alpha i2^{-/-}$, or $G\alpha i3^{-/-}$ mice were stained with 20 μ M CMTMR or 10 μ M CFSE (both dyes from Invitrogen) for 20 min at 37°C, respectively. The labeled cells were mixed at a 1:1 ratio of the two indicated cell types and adoptively transferred by i.v. tail injection of 1×10^7 cells per mouse. The recipient mice were treated by gavage with FTY720 (1 mg/kg) or saline 4 h later, followed by s.c. injection into a hind footpad of 15 μ g anti-LYVE-1 Ab (R&D Systems) conjugated with Alexa Fluor 647 (mAb labeling kit; Invitrogen). The mouse was anesthetized after 16 h and placed on an electrically heated plate to maintain temperature at 36°C. The popliteal lymph node was exposed by small skin incisions and bathed with a continuous flow of warm saline to maintain a local temperature at 36°C during the imaging. Intravital imaging of the lymph node was performed by a home-built microscope, and images were acquired under the control of software developed in-house (19). The in vivo confocal microscope was equipped with three photomultiplier tubes (R9110; Hamamatsu) that were optimized to provide bright images with a high contrast. Each xy-plane spanned 250×250 μ m at a resolution of two pixels per micrometer. Stacks of images were acquired with a z-axis resolution of 3 μ m per section, and time-series images were obtained at a 20-s interval. To determine whether a cell was inside, outside, or on the border of a cortical sinus, each cell located relative to the sinusoid wall was assessed in the xy-plane and/or z-plane. The moving distances and velocities of the tracking cells were tracked for each video segment and calculated using ImageJ software (NIH Image).

Statistical analysis

Statistical tests were performed using one-way ANOVA for multiple group comparisons. A *p* value <0.05 was considered significant.

Results

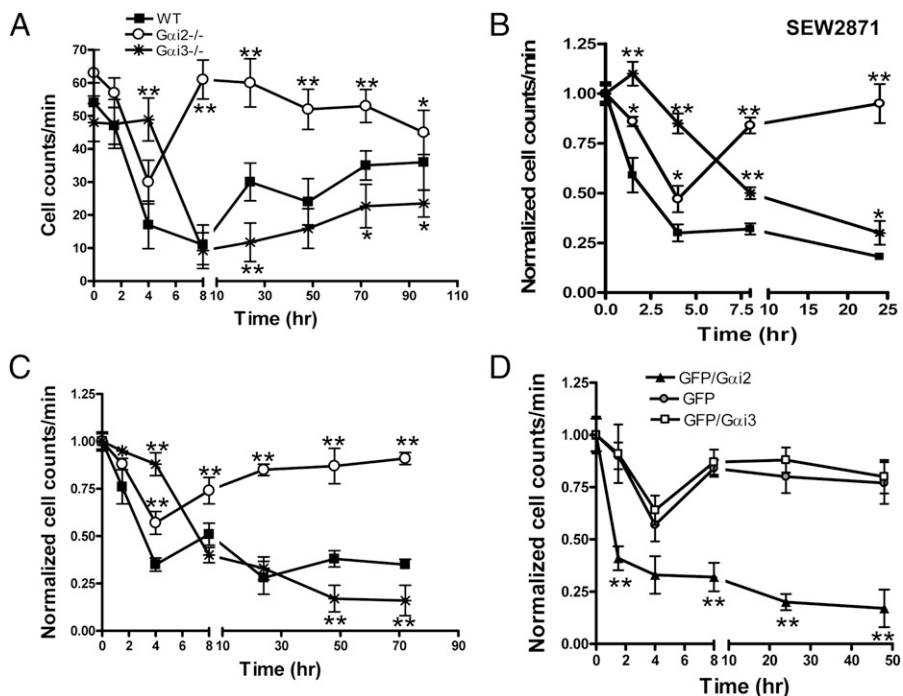
T cells from $G\alpha i2^{-/-}$ mice cannot be sequestered sufficiently by FTY720

To explore whether $G\alpha i2$ and $G\alpha i3$ played a distinct role in FTY720-induced lymphopenia, we tracked the circulation of adoptively transferred $G\alpha i2$ - and $G\alpha i3$ -deficient T cells in real time in a living animal after FTY720 treatment by an in vivo flow cytometer (20). The instrumentation allows detection and quantification of adoptively transferred, fluorescently labeled cells flowing through the same ear vessel in live animals over an extended period of time without the extraction of blood samples because repeated blood draws potentially can cause stress and reduce the number of circulating lymphocytes (20–22). To quantify circulating cells, T cells isolated from WT, $G\alpha i2^{-/-}$, or $G\alpha i3^{-/-}$ mice were labeled with a vital red fluorescent dye before being administered to cognate WT mice and counted 16 h later via the ear vessel to establish control values (Fig. 1, time 0). The donor cells were monitored in the same ear vessel at the indicated times after gavage of the mice with 1 mg/kg FTY720. As shown in Fig. 1A, the number of WT T cells declined precipitously over a 4-h period of time and reached the lowest level at 8 h after FTY720 treatment. $G\alpha i3^{-/-}$ T cells also reached the lowest level at a similar time window, although they were refractory to leaving the circulation for the initial 4 h. The number of $G\alpha i2^{-/-}$ T cells in circulation diminished similar to that of WT T cells in the first 4 h, but it never reached the lowest levels as those numbers seen with WT and $G\alpha i3^{-/-}$ T cells. Rather, $G\alpha i2$ -deficient T cells circulated back to the blood, reached the initial level by 8 h, and remained at the level afterward. In sharp contrast, WT and $G\alpha i3^{-/-}$ T cells were trapped in the tissues, returning to the blood slowly and gradually over a period of 3 d as described previously (23). To rule out that a faster recovery of circulating $G\alpha i2^{-/-}$ T cells after FTY720 treatment resulted from a release of the cells from non-lymphoid tissues such as the lung or liver, the number of circulating T cells was also monitored directly in the lymph. A similar reduction in the number of circulating T cells followed by a faster recovery again was observed in the lymph only in the absence of $G\alpha i2$ (Supplemental Fig. 1A).

Of note, numbers of circulating $G\alpha i2^{-/-}$, $G\alpha i3^{-/-}$, and WT T cells differed at the time of FTY720 administration as well as in saline control mice (Fig. 1A, Supplemental Fig. 1B), even though the same number of cells were adoptively transferred into the mice. An increase in circulating $G\alpha i2^{-/-}$ T cells but a decrease in $G\alpha i3^{-/-}$ T cells relative to WT cells was constantly observed and hinted at a difference between $G\alpha i2$ and $G\alpha i3$ in the regulation of T cell trafficking. For a better comparison of FTY720-induced lymphopenia, the numbers of circulating T cells were normalized to 1 at time 0 in subsequent studies. After the normalization, a slight but significant increase in FTY720-induced sequestration of $G\alpha i3^{-/-}$ T cells still was demonstrated when compared with that of WT T cells (data not shown).

To exclude the possibility that insufficient sequestration of $G\alpha i2^{-/-}$ T cells resulted from overlapping stimulation of other S1P receptors by FTY720, the S1P₁R-specific agonist SEW2871 was tested. Unlike FTY720, which can potentially activate other G proteins besides $G\alpha i2$ or $G\alpha i3$ by binding to additional S1P receptors such as S1P₄R on T cells, SEW2871 induces lymphopenia via exclusive activation of S1P₁R (24). Like FTY720, SEW2871 caused lymphopenia persistently in $G\alpha i3^{-/-}$ and WT T cells but only transiently in $G\alpha i2^{-/-}$ T cells (Fig. 1B). The result suggests the involvement of S1P₁R only in the action of FTY720 in $G\alpha i2^{-/-}$ T cells. Similar results were also attained in reciprocal experiments in which WT, $G\alpha i2^{-/-}$, or $G\alpha i3^{-/-}$

FIGURE 1. FTY720 fails to sequester $G\alpha i2^{-/-}$ T cells in either $G\alpha i2^{-/-}$ or WT recipient mice. *A–D*, T cells from the indicated mice were stained with DiD, except for *D*, and injected into cognate WT mice (*A, B, D*) or $G\alpha i2^{-/-}$ mice (*C*). $G\alpha i2$ -deficient T cells were infected with a GFP-lentivirus (GFP) or the lentivirus constructed with $G\alpha i2$ (GFP/ $G\alpha i2$) or $G\alpha i3$ (GFP/ $G\alpha i3$) in *D*. The recipients were treated with 1 mg/kg FTY720 once (*A, C, D*) or 10 mg/kg SEW2871 every 12 h (*B*). Fluorescently labeled cells in circulation were counted by in vivo flow cytometer at the indicated time points. The data represent means \pm SD of cell counts per minute of six separate experiments for *A* or three separate experiments for *B–D*. * $p < 0.05$, ** $p < 0.01$, respectively, in presence or absence of $G\alpha i2$ or $G\alpha i3$.



T cells were introduced into $G\alpha i2^{-/-}$ mice (Fig. 1C) or $G\alpha i3^{-/-}$ mice (data not shown), with only $G\alpha i2^{-/-}$ T cells remaining in the circulation after FTY720 administration. Clearly, a defect in T cells rather than endothelial cells ablated FTY720-induced lymphopenia in the absence of $G\alpha i2$.

Moreover, an insufficient response of $G\alpha i2^{-/-}$ T cells to FTY720 was also unlikely to be caused by altered T cell differentiation in the absence of $G\alpha i2$ because previous studies showed normal T cell development in the animal (15, 25). To further corroborate this, $G\alpha i2$ expression was restored to a WT level in the cells by the infection of the cells with a GFP-lentivirus constructed with $G\alpha i2$ or $G\alpha i3$ or a control GFP-lentivirus as shown in Supplemental Fig. 1C. The infected cells were administered to cognate WT mice and counted before and after FTY720 treatment as above. $G\alpha i2^{-/-}$ T cells responded to FTY720-mediated sequestration normally after infection with $G\alpha i2$ /GFP-lentivirus but not with $G\alpha i3$ /GFP-lentivirus or control GFP-lentivirus (Fig. 1D). The ability of ectopic $G\alpha i2$ expression to restore FTY720 responses in the cells unambiguously confirms that a loss of $G\alpha i2$ in $S1P_1R$ -mediated signaling is directly responsible for the insufficient response of $G\alpha i2^{-/-}$ T cells to FTY720.

Similar downregulation of $S1P_1R$ on T cells in the presence or absence of $G\alpha i2$

FTY720 has long been shown to induce internalization of $S1P_1R$ on T cells, abolishing $S1P$ -mediated chemotaxis and thus egress of the cells (4–7). Lack of $G\alpha i2$ might abrogate FTY720-induced receptor internalization, rendering the cells refractory to FTY720-induced lymphopenia. To address this, the level of $S1P_1R$ expression was analyzed on lymph node T cells isolated from FTY720-treated and nontreated mice by a polyclonal Ab specific for the N-terminal 49 amino acid residues of mouse $S1P_1R$ as described (7). It was found that $S1P_1R$ expression diminished indiscriminately to background levels in the presence or absence of $G\alpha i2$ in 16 h after gavage of 1 mg/kg FTY720 (Fig. 2). Similar receptor modulation in these three groups of T cells was also observed after 44 or 66 h of FTY720 treatment (data not shown). The result confirms that $G\alpha i2^{-/-}$ T cells exit lymph nodes independent of the cell surface $S1P_1R$ receptor.

Egress of $G\alpha i2^{-/-}$ T cells in FTY720-treated mice was not ascribed to altered cell motility

Cell motility was tracked by real-time imaging of the popliteal lymph node in WT mice receiving equal numbers of fluorescently labeled T cells prepared from $G\alpha i2^{-/-}$ or $G\alpha i3^{-/-}$ and WT mice (19). The average velocities of $G\alpha i3^{-/-}$ and WT T cells were comparable in control mice and were not altered significantly after FTY720 treatment (Supplemental Fig. 2A). Unexpectedly, the velocity of $G\alpha i2^{-/-}$ T cells decreased, rather than increased, by $\sim 20\%$ compared with that of WT or $G\alpha i3^{-/-}$ T cells in the distal area of the cortical sinus, irrespective of FTY720 treatment (Supplemental Fig. 2A), similar to that described with $G\alpha i2^{-/-}$ B cells (8). A decrease in the velocity of $G\alpha i2$ -deficient T cells was also described previously (26) and might be associated with an impaired response to retention chemokines like SDF-1 as shown in our previous study (13). Superimposed tracking of 20 randomly selected cells of each phenotype over 15 min confirmed similar tracks for $G\alpha i3^{-/-}$ and WT T cells but less vigorous

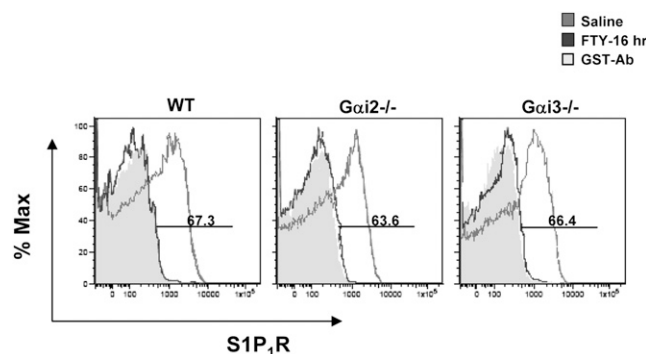


FIGURE 2. FTY720 induces $S1P_1R$ internalization in the presence or absence of $G\alpha i2$. Mice with the indicated phenotypes were treated with 1 mg/kg FTY720 or saline. Lymph node cells were isolated from saline- and FTY720-treated mice at 16 h posttreatment and stained with anti- $S1P_1R$ Ab or control Ab against GST (shaded area). Representative flow cytometric profiles are shown where the numbers indicate the percentages of $S1P_1R^+$ cells on gated $CD3^+$ T cells.

movement of $G\alpha i2^{-/-}$ T cells, in particular, in the presence of FTY720 (Supplemental Fig. 2B). The decreased motility superficially contradicted sufficient egress of $G\alpha i2^{-/-}$ T cells in FTY720-treated mice.

$G\alpha i2^{-/-}$ T cells enter, but WT T cells depart, the cortical sinus in the presence of FTY720

We then tracked T cell behavior around cortical sinusoids of lymphoid nodes, because these structures were identified recently to be sites for T cell egress (8, 9). We found no significant difference in the distribution of T cells lacking either $G\alpha i2$ or $G\alpha i3$ protein inside and outside cortical sinusoids in control mice (Fig. 3A–C). Enumeration of ~600 cells inside the sinusoids in 20–30 randomly selected imaging stacks collected from six lymph nodes revealed that average numbers of WT, $G\alpha i2^{-/-}$, and $G\alpha i3^{-/-}$ T cells were similar in these regions (Fig. 3A–C, 3G). Likewise, the numbers of $G\alpha i2^{-/-}$, $G\alpha i3^{-/-}$, and WT T cells within 30 μm of each cortical sinus were comparable (Fig. 3A–C, 3H) (8). However, there were

few WT or $G\alpha i3^{-/-}$ T cells (red) in sinusoid lumens after FTY720 administration (Fig. 3D–G). In sharp contrast, the number of $G\alpha i2^{-/-}$ T cells inside the sinuses remained almost identical to that in control mice (Fig. 3D, 3F, 3G). Clearly, $G\alpha i2^{-/-}$ T cells exit lymph nodes in FTY720-treated animals through the same anatomic structure. Also noticed was a strong bias in the number of $G\alpha i2^{-/-}$ T cells (green) in the surrounding area (<30 μm) of sinusoids as delineated by a dotted yellow line in mice receiving $G\alpha i2^{-/-}$ T cells and WT or $G\alpha i3^{-/-}$ T cells (Fig. 3D, 3F, 3H; $p < 0.001$). The ability of $G\alpha i2^{-/-}$ T cells to enter the sinus sufficiently, concurrent with a drastic decrease in the entry of WT or $G\alpha i3^{-/-}$ T cells, gave rise to a majority of $G\alpha i2^{-/-}$ T cells and a scant fraction of WT or $G\alpha i3^{-/-}$ T cells inside sinusoids in FTY720-treated mice (Fig. 3D, 3F, 3G; $p < 0.001$). These imaging studies demonstrate a similar behavior between WT and $G\alpha i3^{-/-}$ T cells and distinct behavior between $G\alpha i2^{-/-}$ and $G\alpha i3^{-/-}$ or WT cells in the vicinity of the sinus in FTY720-treated mice, in agreement with *in vivo* flow cytometric analysis (Fig. 1).

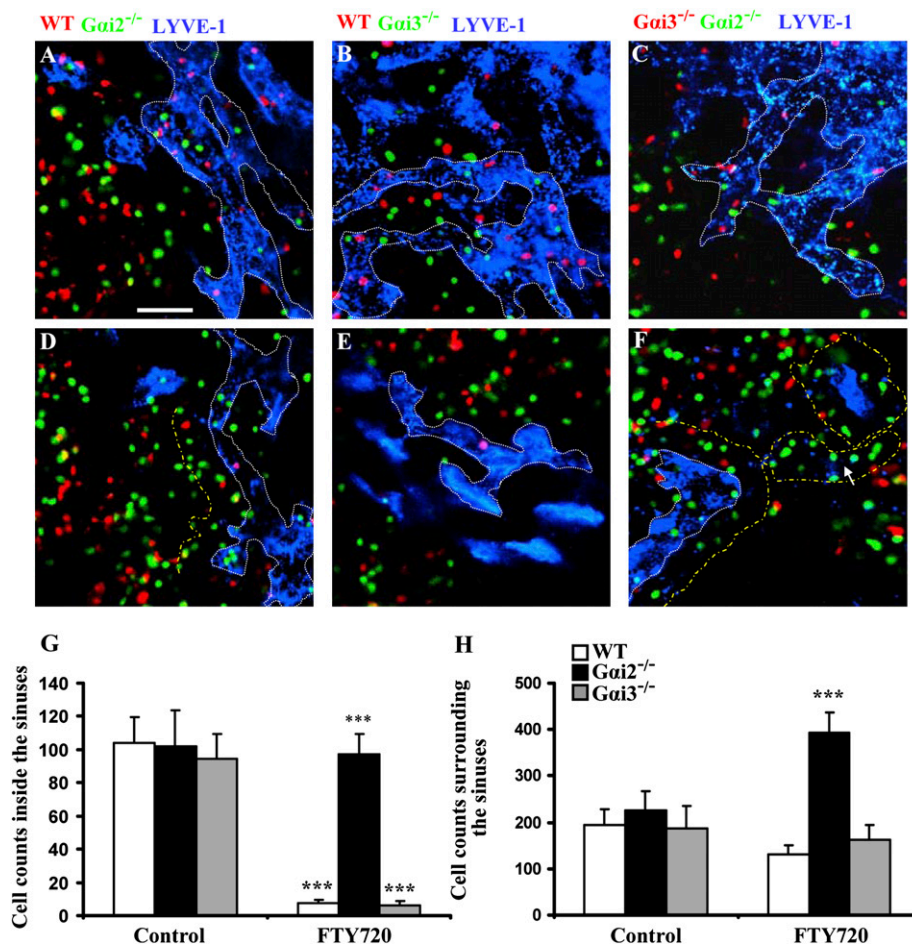


FIGURE 3. Entry of only $G\alpha i2^{-/-}$ T cells into the cortical sinus in FTY720-treated mice. A–F, Equal numbers of CMTMR-labeled WT or $G\alpha i3^{-/-}$ T cells (red) and CFSE-labeled $G\alpha i2^{-/-}$ T cells (green) were administered *i.v.* to cognate WT mice. The recipient mice were treated by gavage 4 h later with FTY720 or vehicle, followed by *s.c.* injection of Alexa Fluor 647-conjugated anti-LYVE-1 Ab in a hind footpad. The cortical sinusoid region in and adjacent to T cell zones of the popliteal lymph node was imaged 16 h later by intravital confocal microscopy. The representative images were taken from control (A–C) or FTY720-treated (D–F) mice receiving WT and $G\alpha i2^{-/-}$ T cells (A, D) or $G\alpha i3^{-/-}$ T cells (B, E) or $G\alpha i3^{-/-}$ and $G\alpha i2^{-/-}$ T cells (C, F), respectively. LYVE-1⁺ cortical sinuses are shown in blue pseudocolor to distinguish them from red cells, and the representative sinus area is delineated by a dotted white line. The dotted yellow line in D and F outlines the area within 30 μm of the outer boundaries of cortical sinuses at either the *xy*-plane or the *z*-plane (arrow in F) where there is a branch of the sinus underneath the green cells. Note that more $G\alpha i2^{-/-}$ T cells than WT or $G\alpha i3^{-/-}$ T cells are around sinusoids in FTY720-treated mice (D, F). The data are representative of three separate experiments with two lymph nodes imaged in each mouse. Scale bar, 50 μm . G and H, Averages of WT, $G\alpha i2^{-/-}$, and $G\alpha i3^{-/-}$ donor T cells inside (G) or in a 30- μm -thick area surrounding (H) the cortical sinuses per control and FTY720-treated lymph node were attained by enumeration of 600 cells in 20–30 randomly selected imaging stacks from each lymph node. Data shown are the mean \pm SEM of 600 cells tracked from three separate experiments with two lymph nodes imaged in each mouse. *** $p < 0.001$ in the presence or absence of $G\alpha i2$ or FTY720.

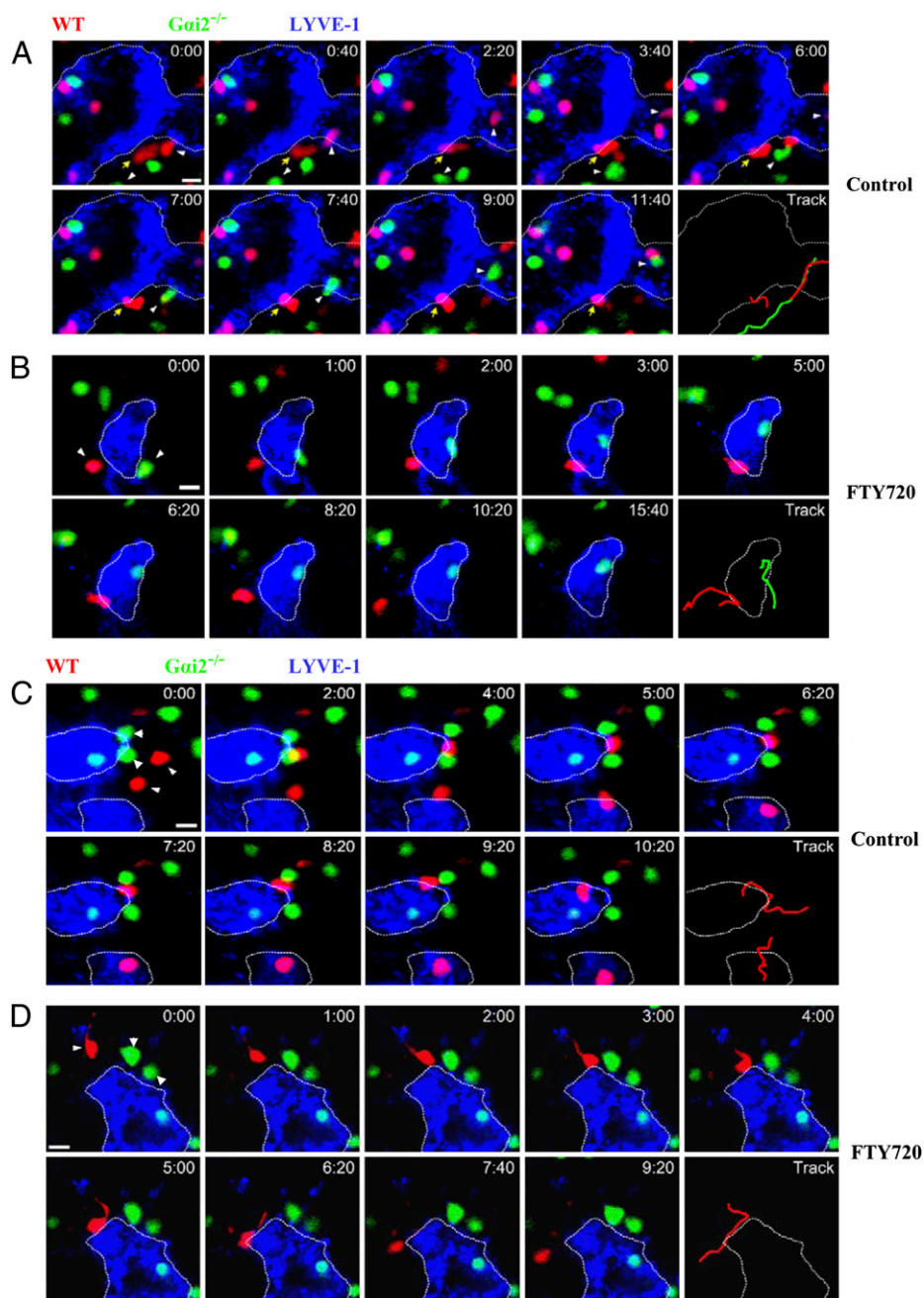
Increased adhesion of G α i2^{-/-} T cells to the sinusoid surface

To identify a potential difference between WT and G α i2^{-/-} T cells in their abilities to approach, engage, crawl along, and retract from the cortical sinus in control and FTY720-treated mice, time-series images of individual cells were enlarged and traced. Representative images are shown in Fig. 4 in which one WT cell (red, white arrow), followed by a G α i2^{-/-} cell (green, white arrow), approached and entered a sinusoid by the same exit site in control mice (Fig. 4A). Another WT cell (yellow arrow) approached, adhered, and then protruded its leading edge into the sinus before entry. Likewise, two WT cells approached and engaged different sinusoids for ~7 or 3 min, respectively, and established adhesion on the sinus before they successfully crossed the sinusoid wall in control mice (Fig. 4C, Supplemental Video 1). In sharp contrast, WT cells approached, engaged, and sometimes even extended a process into the sinus but retracted and went away in FTY720-

treated mice (Fig. 4B, 4D, arrowhead, Supplemental Videos 2, 3). Although the drug drastically altered the behavior of WT cells, it appeared to have little impact on G α i2^{-/-} T cells. As can be seen in Fig. 1B, a G α i2^{-/-} T cell adhered to the sinusoid, polarized, and penetrated into it in the presence of FTY720 (Supplemental Videos 2, 4). We observed only occasionally G α i2^{-/-} T cells migrating away from the sinus during the imaging study. In many cases, G α i2^{-/-} T cells adhered to a specific site on the sinusoid surface so strongly that they could not be pulled away despite vigorous motion of their pseudopodia for several minutes (Fig. 4D, arrowheads, Supplemental Movies 3, 4).

Enhanced adhesion of G α i2^{-/-} T cells to the sinusoid surface was illustrated further by analyzing 20 randomly selected WT cells and an equal number of G α i2^{-/-} cells that were either already adhered to the sinus when the recording started or migrating toward and subsequently engaging the sinus in the same region during a 25-min recording period of time. Among the 20

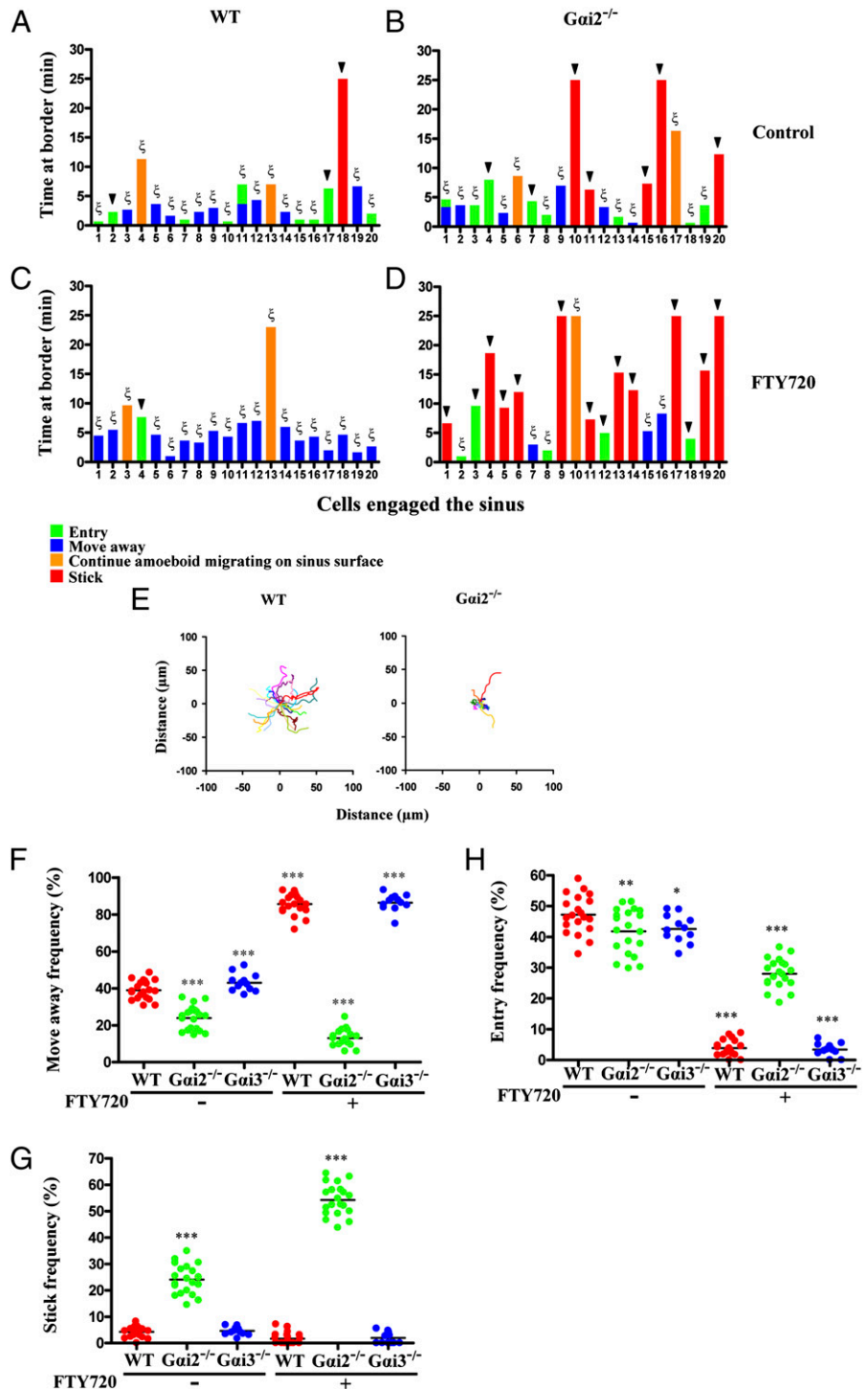
FIGURE 4. Distinct behaviors of T cells after they approach the sinus in the presence or absence of G α i2. *A–D*, Time-lapse images of individual WT and G α i2^{-/-} cells prepared in Fig. 3 were enlarged and tracked for their behavior on and around the sinus in mice treated with vehicle (*A, C*) and FTY720 (*B, D*). Note that the two WT T cells departing in *B* and *D* kept amoeboid migration on the sinus without establishment of sufficient adhesion to it (Supplemental Videos 2, 3). Elapsed times are presented as minutes:seconds, sinus boundaries are outlined by a dotted white line, and arrowheads indicate the cells that are tracked. Additional images are provided in Supplemental Videos 1–5. The cumulative cell trajectories throughout the imaging period are shown as a red line for WT T cells and a green line for G α i2^{-/-} T cells in the last panel of every time-lapse image series. Scale bars, 10 μ m. Similar results were obtained with three independent experiments.



WT cells traced, 9 of them entered and 8 moved away from the sinus in control mice, indicating a balance between sinus-away and sinus-entry signals under a physiological condition (Fig. 5A). This probably also held truth for $G\alpha i2^{-/-}$ T cells in which 8 cells entered and 5 cells departed, albeit at a reduced rate in either direction (Fig. 5B). The diminished rate of both sinus-away and sinus-entry movement brought about a greater number of $G\alpha i2^{-/-}$ cells remaining on the sinus than WT cells (Fig. 5B versus Fig. 5A), with 7 $G\alpha i2^{-/-}$ cells firmly adherent on the sinus for more than 2 min without displacement, in contrast to only 3 WT cells sticking on the sinus (Fig. 5A, 5B). The number of $G\alpha i2^{-/-}$ cells sticking on the sinus further increased to 14 in the presence of

FTY720 (Fig. 5D). However, an opposite trend was seen in the presence of $G\alpha i2$, with only one WT cell (fourth cell in Fig. 5C) adhering to the sinus, and this was the cell that was able to enter the sinus (Fig. 5C). Remarkably, none of the cells that formed sufficient adhesion on the sinus, as marked in black arrowheads, migrated away, regardless of $G\alpha i2$ expression, and all of them were able to enter the sinus in the presence or absence of FTY720. The observation argues that the formation of an anchor between T cells and the sinus may be required to “stop” the sinus-away signal and to acquire a polarized cell shape for them squeezing into the sinus. Thus, a failure to establish sufficient interactions between T cells and sinuses robustly increased the number (17) of

FIGURE 5. Lack of $G\alpha i2$ facilitates adhesion of T cells to the sinusoid surface. *A–D*, The time spent by individual donor T cells that remained on the outer border of the cortical sinuses and their subsequent movements were compared between control (*A, B*) and FTY720-treated (*C, D*) mice. The time in which cells engaged and entered the sinuses is indicated in green, whereas the duration during which cells crawled on the sinus but failed to cross and then moved away is indicated in blue. The red bars indicate the times in which a cell adhered to the same site on the sinus without displacement until the end of imaging; the orange bars are durations during which a cell kept amoeboid migrating on the sinus; arrowheads indicate the cells that adhered to a single point on the sinus for longer than 2 min regardless of whether they crossed the sinus; and “ξ” indicates cells that never adhered to the sinus for longer than 2 min after they engaged the sinus. The data are representative of three independent experiments. *E*, T cell migration on the surface of the cortical sinus in the presence or absence of $G\alpha i2$ in FTY720-treated mice. Superimposed tracks of 20 randomly selected WT or $G\alpha i2^{-/-}$ donor T cells were recorded when the cells began engagement of the sinus and ended when the cells left in FTY720-treated recipient mice. The data are representative of images collected from six lymph nodes in each treatment. *F–H*, Frequencies at which WT, $G\alpha i2^{-/-}$, or $G\alpha i3^{-/-}$ donor T cells moved away (*F*), adhered to (*G*), or entered (*H*) the cortical sinus in control and FTY720-treated mice were calculated by manually tracking individual cells in each time-lapse image, with a total of 400 cells in 20 imaging stacks. Adhesion was defined as a cell adhered to a single point on the sinusoid surface without displacement for longer than 2 min. Each dot represents data from a single time-lapse image, and the lines represent the means. The data are collected from six lymph nodes imaged in each treatment. * $p < 0.05$, ** $p < 0.01$, *** $p < 0.001$ in the presence or absence of $G\alpha i2$ or FTY720.



WT T cells departing the sinus, preventing their egress (Fig. 5C). However, a lack of G α i2 strengthened T cell adhesion to the sinusoid surface, which prevented their migration away and facilitated their transmigration of the sinusoids (Fig. 5D). A few G α i2^{-/-} T cells did not establish adhesion on the sinusoid surface and departed in the presence of FTY720 (Fig. 5D, Supplemental Video 5). A blockade of T cell–sinus interactions by FTY720 was consistent with vigorous movement of the cells over the sinusoid surface, which was reflected by superimposed tracking of 20 randomly selected WT T cells (Fig. 5E). The unrestricted migratory paths were in sharp contrast to the locally confined migration seen in most G α i2^{-/-} T cells.

Tracking of 400 cells from 20 samples, except for G α i3^{-/-} T cells in which 12 samples were analyzed, further corroborated an inverse relationship between sinus-away migration and adhesive responses in both the presence and the absence of FTY720 (Fig. 5F versus Fig. 5G). The frequency of WT or G α i3^{-/-} T cells departing the sinus increased from 39 or 43% in the absence of FTY720 to 85 or 86% in the presence of the drug (Fig. 5F), with only a few cells remaining on the sinus (Fig. 5G), conferring very few chances for the cells to exit (Fig. 5H). On the contrary, the drug greatly enhanced the adhesion of G α i2^{-/-} T cells on the sinus (Fig. 5G), concomitant with a sharp decrease in the number of cells migrating away (Fig. 5F). The enhanced adhesion was in a good agreement with their reduced motility on or around the sinus (Fig. 5E). Despite their ability to enter the sinus, G α i2^{-/-} T cells transmigrated the sinusoids at a significantly low level in the presence of FTY720 compared with that in the absence of FTY720 (Fig. 5H), presumably owing to S1P₁R receptor internalization. The diminished transmigration might be responsible for an initial decline in the number of circulating G α i2^{-/-} T cells (<4 h) after FTY720 treatment (Fig. 1). In support of a role for S1P-induced chemotaxis in T cell egress, G α i2- and G α i3-deficient T cells entered the sinus at an efficiency slightly lower than that of WT cells in the control mice (Fig. 5H, $p < 0.01$ or 0.05, respectively), which is consistent with the slightly reduced chemotaxis induced by S1P in these cells described previously (14). The reduced entry of G α i2^{-/-} T cells into the sinus might be compensated eventually by an increasing number of cells adherent on the sinus, resulting in the normalization of circulating G α i2^{-/-} T cells in 8 h after FTY720 treatment (Fig. 1). The results suggest that both receptor internalization and enhanced sinus-away migration contribute to FTY720-induced sequestration of T cells in the lymphoid tissue.

Discussion

The investigation reveals, for the first time, to our knowledge, the possible involvement of T cell adhesion on the sinus for regulating egress of lymphocytes, in a good agreement with a multistep model of T cell egress that requires S1P₁R-independent probing of the sinus before S1P-guided entry (27). The role of T cell adhesion to the sinus in intravasation may be similar to that in extravasation. During the process of extravasation, leukocytes adhere to endothelial cells or extracellular matrix, a process by which they stop a shear force and acquire a polarized cell shape enabling them to squeeze into the tissues through a vessel wall. Sticking of T cells on the sinusoid surface appeared to “stop” the tissue-retention or sinus-away signal in favor of T cells transmigrating across the sinus during T cell egress. The importance of halting the sinus-away signal for T cell egress is underscored by the observation that none of the cells that had formed firm adhesion on the sinus moved away in the presence or absence of FTY720. On the basis of these observations and published data, we propose a model for T cell egress as depicted in Supplemental Fig. 3. T cells crawl

along chemokine-decorated fiber paths generated by fibroblastic reticular cells in the T cell zone, approach, and engage the sinus (28), after which T cells adhere to the sinus that prohibits the cells from migrating away. The adhesion is followed presumably by deadhesion and entry of the cells into the sinus after the cue of S1P. This process is likely to take place quickly in most of cells under physiological conditions and thus may not be captured readily by imaging studies. FTY720 impairs the adhesion or accelerates deadhesion, permitting relatively unrestricted migration of the cells along or away from the sinus, as reflected by vigorous movements of WT cells on the sinusoid surface and frequent retraction to the parenchyma even after they protrude their leading edges into the sinus. In the absence of G α i2, FTY720 treatment strengthens the adhesion that stops the sinus-away signal and promotes T cells entry to the sinus with or without the S1P cue (Supplemental Fig. 3, lower panel), although the underlying mechanism remains unknown. Ligation of S1P₁R has been shown to activate integrin-mediated firm arrest in high endothelial venules (29). The adhesion molecules involved in this intravasation are not known at present, which are presumably different from those adhesion molecules and selectins such as α _L β ₂ (LFA-1 or CD11a/CD18), α ₄ β ₁ (VLA-4), and L-selectin for diapedesis or S1P₁R-induced tissue retention in the skin (30) because sticking of G α i2^{-/-} T cells occurs only on the surface of the sinus in the presence or absence of FTY720. Moreover, injection of neutralizing Abs against integrins such as α _L, α ₄, or β ₂ did not reveal any role for these integrins in lymphocyte egress from secondary lymph organs (7, 31). G α i2-deficient T cells may provide us with a unique opportunity to unravel the nature of the adhesion molecules involved in T cell egress because of their extended adhesion on the sinus.

S1P₁R has been shown to exclusively couple with PTX-sensitive heterotrimeric G α i/o proteins (10). T cells express only G α i2 and G α i3, and no G α i1 or G α o is expressed to compensate for a loss of either G α i protein in G α i2- and G α i3-deficient mice as analyzed by RT-PCR (data not shown) (32). These two G α i proteins were thought to be redundant in coupling to S1P₁R, because G α i2- and G α i3-deficient T cells both displayed similar chemotactic responses to S1P, albeit to a slightly lower degree compared with that of WT cells (14). T cell egress and emigration of thymocytes were normal in these two strains of mice (16). Binding of FTY720 to S1P₁R also induced S1P₁R internalization on these three groups of cells but sequestered WT and G α i3^{-/-} T cells not G α i2^{-/-} T cells. The importance of G α i2 in FTY720-stimulated sequestration was implicated strongly by restoring the response in G α i2-deficient T cells after ectopic G α i2 expression. Mullershausen et al. (33) recently showed long persistent signaling induced by phosphorylated FTY720 after S1P₁R internalization in Chinese hamster ovary cells expressing S1P₁R or primary HUVECs. Persistent activation of G α i2 proteins by internalized S1P₁R may play a critical role in the abrogation of T cell and sinusoid interaction, probably in part through the inhibition of cAMP production, in light of the importance of cAMP in cell–cell adhesion and the well-documented cAMP inhibitory activity of G α i (34), which is currently under investigation.

Our study also provides compelling evidence demonstrating that FTY720 modulation of T cell egress is attributed directly to its action on T cells rather than endothelial cells and that FTY720 does not close the lymphatic endothelial “stromal portal,” if it exists (35). Hence, FTY720 could not block egress of G α i2^{-/-} T cells, irrespective of whether the cells were adoptively transferred into WT or G α i2^{-/-} mice. Its action is also unlikely via other S1P receptors, other than the S1P₁R, because SEW2871 that is specific for the S1P₁R cannot inhibit egress of G α i2^{-/-} T cells either.

Moreover, restoration of FTY720-mediated responses in $\text{G}\alpha\text{i}2^{-/-}$ T cells after the transfection of $\text{G}\alpha\text{i}2$, but not $\text{G}\alpha\text{i}3$, into the cells corroborated that failure of FTY720 to sequester $\text{G}\alpha\text{i}2^{-/-}$ T cells in the secondary lymphoid tissues did not result from a developmental defect in the cells (Fig. 1D). Consistent with this was our early study showing that thymic emigration of T cells was normal in $\text{G}\alpha\text{i}2^{-/-}$ mice despite an increase in the number of $\text{CD}4^+$ and $\text{CD}8^+$ cells in the thymus (25). The latter was attributed to an accelerated transition from double-positive to single-positive thymocytes (25). There was also no significant alteration in T cell distribution in $\text{G}\alpha\text{i}2^-$ and $\text{G}\alpha\text{i}3^-$ deficient mice at adulthood, despite a defect in newborn mice in the absence of either $\text{G}\alpha\text{i}2$ or $\text{G}\alpha\text{i}3$ (16).

The current investigation demonstrates that FTY720 blocks egress of T cells by abrogation of T cell and sinusoid interactions in addition to the induction of $\text{S1P}_1\text{R}$ internalization. These novel mechanistic insights into T cell egress can potentially serve as a basis for identifying new therapeutic targets.

Acknowledgments

We thank the members of Dr. Wu's group for stimulating discussion, Dr. Volker Brinkmann at Novartis Pharma AG for phosphorylated FTY720 and FTY720, and Dr. Lutz Birnbaumer for $\text{G}\alpha\text{i}2^{-/-}$ and $\text{G}\alpha\text{i}3^{-/-}$ mice.

Disclosures

The authors have no financial conflicts of interest.

References

- Brinkmann, V., A. Billich, T. Baumruker, P. Heining, R. Schmouder, G. Francis, S. Aradhye, and P. Burtin. 2010. Fingolimod (FTY720): discovery and development of an oral drug to treat multiple sclerosis. *Nat. Rev. Drug Discov.* 9: 883–897.
- Brinkmann, V., J. G. Cyster, and T. Hla. 2004. FTY720: sphingosine 1-phosphate receptor-1 in the control of lymphocyte egress and endothelial barrier function. *Am. J. Transplant.* 4: 1019–1025.
- Luo, Z. J., T. Tanaka, F. Kimura, and M. Miyasaka. 1999. Analysis of the mode of action of a novel immunosuppressant FTY720 in mice. *Immunopharmacology* 41: 199–207.
- Matloubian, M., C. G. Lo, G. Cinamon, M. J. Lesneski, Y. Xu, V. Brinkmann, M. L. Allende, R. L. Proia, and J. G. Cyster. 2004. Lymphocyte egress from thymus and peripheral lymphoid organs is dependent on S1P receptor 1. *Nature* 427: 355–360.
- Gräler, M. H., and E. J. Goetzl. 2004. The immunosuppressant FTY720 downregulates sphingosine 1-phosphate G-protein-coupled receptors. *FASEB J.* 18: 551–553.
- Hale, J. J., W. Neway, S. G. Mills, R. Hajdu, C. Ann Keohane, M. Rosenbach, J. Milligan, G. J. Shei, G. Chrebet, J. Bergstrom, et al. 2004. Potent S1P receptor agonists replicate the pharmacologic actions of the novel immune modulator FTY720. *Bioorg. Med. Chem. Lett.* 14: 3351–3355.
- Lo, C. G., Y. Xu, R. L. Proia, and J. G. Cyster. 2005. Cyclical modulation of sphingosine-1-phosphate receptor 1 surface expression during lymphocyte recirculation and relationship to lymphoid organ transit. *J. Exp. Med.* 201: 291–301.
- Sinha, R. K., C. Park, I. Y. Hwang, M. D. Davis, and J. H. Kehrl. 2009. B lymphocytes exit lymph nodes through cortical lymphatic sinusoids by a mechanism independent of sphingosine-1-phosphate-mediated chemotaxis. *Immunity* 30: 434–446.
- Pham, T. H., T. Okada, M. Matloubian, C. G. Lo, and J. G. Cyster. 2008. S1P_1 receptor signaling overrides retention mediated by G αi coupled receptors to promote T cell egress. *Immunity* 28: 122–133.
- Rosen, H., and E. J. Goetzl. 2005. Sphingosine 1-phosphate and its receptors: an autocrine and paracrine network. *Nat. Rev. Immunol.* 5: 560–570.
- Beals, C. R., C. B. Wilson, and R. M. Perlmutter. 1987. A small multigene family encodes Gi signal-transduction proteins. *Proc. Natl. Acad. Sci. USA* 84: 7886–7890.
- Kim, S. Y., S. L. Ang, D. B. Bloch, K. D. Bloch, Y. Kawahara, C. Tolman, R. Lee, J. G. Seidman, and E. J. Neer. 1988. Identification of cDNA encoding an additional α subunit of a human GTP-binding protein: expression of three α subtypes in human tissues and cell lines. *Proc. Natl. Acad. Sci. USA* 85: 4153–4157.
- Thompson, B. D., Y. Jin, K. H. Wu, R. A. Colvin, A. D. Luster, L. Birnbaumer, and M. X. Wu. 2007. Inhibition of G $\alpha\text{i}2$ activation by G $\alpha\text{i}3$ in CXCR3-mediated signaling. *J. Biol. Chem.* 282: 9547–9555.
- Jin, Y. Z., B. D. Thompson, Z. Y. Zhou, Y. Fu, L. Birnbaumer, and M. X. Wu. 2008. Reciprocal function of Galphai2 and Galphai3 in graft-versus-host disease. *Eur. J. Immunol.* 38: 1988–1998.
- Rudolph, U., M. J. Finegold, S. S. Rich, G. R. Harriman, Y. Srinivasan, P. Brabet, G. Boulay, A. Bradley, and L. Birnbaumer. 1995. Ulcerative colitis and adenocarcinoma of the colon in G $\alpha\text{i}2$ -deficient mice. *Nat. Genet.* 10: 143–150.
- Jin, Y., and M. X. Wu. 2008. Requirement of Galphai in thymic homing and early T cell development. *Mol. Immunol.* 45: 3401–3410.
- Wu, M. X., J. F. Daley, R. A. Rasmussen, and S. F. Schlossman. 1995. Monocytes are required to prime peripheral blood T cells to undergo apoptosis. *Proc. Natl. Acad. Sci. USA* 92: 1525–1529.
- Sanna, M. G., J. Liao, E. Jo, C. Alfonso, M. Y. Ahn, M. S. Peterson, B. Webb, S. Lefebvre, J. Chun, N. Gray, and H. Rosen. 2004. Sphingosine 1-phosphate (S1P) receptor subtypes S1P_1 and S1P_3 , respectively, regulate lymphocyte recirculation and heart rate. *J. Biol. Chem.* 279: 13839–13848.
- Kim, P., M. Puoris'haag, D. Côté, C. P. Lin, and S. H. Yun. 2008. In vivo confocal and multiphoton microendoscopy. *J. Biomed. Opt.* 13: 010501.
- Novak, J., I. Georgakoudi, X. Wei, A. Prossin, and C. P. Lin. 2004. In vivo flow cytometry for real-time detection and quantification of circulating cells. *Opt. Lett.* 29: 77–79.
- Georgakoudi, I., N. Solban, J. Novak, W. L. Rice, X. Wei, T. Hasan, and C. P. Lin. 2004. In vivo flow cytometry: a new method for enumerating circulating cancer cells. *Cancer Res.* 64: 5044–5047.
- Dhabhar, F. S., A. H. Miller, B. S. McEwen, and R. L. Spencer. 1995. Effects of stress on immune cell distribution. Dynamics and hormonal mechanisms. *J. Immunol.* 154: 5511–5527.
- Mandala, S., R. Hajdu, J. Bergstrom, E. Quackenbush, J. Xie, J. Milligan, R. Thornton, G. J. Shei, D. Card, C. Keohane, et al. 2002. Alteration of lymphocyte trafficking by sphingosine-1-phosphate receptor agonists. *Science* 296: 346–349.
- Jo, E., M. G. Sanna, P. J. Gonzalez-Cabrera, S. Thangada, G. Tigyi, D. A. Osborne, T. Hla, A. L. Parrill, and H. Rosen. 2005. S1P_1 -selective in vivo-active agonists from high-throughput screening: off-the-shelf chemical probes of receptor interactions, signaling, and fate. *Chem. Biol.* 12: 703–715.
- Zhang, Y., M. J. Finegold, Y. Jin, and M. X. Wu. 2005. Accelerated transition from the double-positive to single-positive thymocytes in G $\alpha\text{i}2$ -deficient mice. *Int. Immunol.* 17: 233–243.
- Hwang, I. Y., C. Park, and J. H. Kehrl. 2007. Impaired trafficking of $\text{Gnai}2^+/-$ and $\text{Gnai}2^-/-$ T lymphocytes: implications for T cell movement within lymph nodes. *J. Immunol.* 179: 439–448.
- Grigorova, I. L., S. R. Schwab, T. G. Phan, T. H. Pham, T. Okada, and J. G. Cyster. 2009. Cortical sinus probing, S1P_1 -dependent entry and flow-based capture of egressing T cells. *Nat. Immunol.* 10: 58–65.
- Bajénoff, M., J. G. Egen, L. Y. Koo, J. P. Laugier, F. Brau, N. Glaichenhaus, and R. N. Germain. 2006. Stromal cell networks regulate lymphocyte entry, migration, and territoriality in lymph nodes. *Immunity* 25: 989–1001.
- Halin, C., M. L. Scimone, R. Bonasio, J. M. Gauguier, T. R. Mempel, E. Quackenbush, R. L. Proia, S. Mandala, and U. H. von Andrian. 2005. The S1P -analog FTY720 differentially modulates T-cell homing via HEV: T-cell-expressed S1P_1 amplifies integrin activation in peripheral lymph nodes but not in Peyer patches. *Blood* 106: 1314–1322.
- Ledgerwood, L. G., G. Lal, N. Zhang, A. Garin, S. J. Esses, F. Ginhoux, M. Merad, H. Peche, S. A. Lira, Y. Ding, et al. 2008. The sphingosine 1-phosphate receptor 1 causes tissue retention by inhibiting the entry of peripheral tissue T lymphocytes into afferent lymphatics. *Nat. Immunol.* 9: 42–53.
- Arnold, C. N., E. C. Butcher, and D. J. Campbell. 2004. Antigen-specific lymphocyte sequestration in lymphoid organs: lack of essential roles for αL and α4 integrin-dependent adhesion or Galphai protein-coupled receptor signaling. *J. Immunol.* 173: 866–873.
- Huang, T. T., Y. Zong, H. Dalwadi, C. Chung, M. C. Miceli, K. Spicher, L. Birnbaumer, J. Braun, and R. Aranda. 2003. TCR-mediated hyper-responsiveness of autoimmune Galphai2(-/-) mice is an intrinsic naïve $\text{CD}4^+$ T cell disorder selective for the Galphai2 subunit. *Int. Immunol.* 15: 1359–1367.
- Mullershausen, F., F. Zecri, C. Cetin, A. Billich, D. Guerini, and K. Seuwen. 2009. Persistent signaling induced by FTY720-phosphate is mediated by internalized S1P_1 receptors. *Nat. Chem. Biol.* 5: 428–434.
- Lorenowicz, M. J., M. Fernandez-Borja, and P. L. Hordijk. 2007. cAMP signaling in leukocyte transendothelial migration. *Arterioscler. Thromb. Vasc. Biol.* 27: 1014–1022.
- Wei, S. H., H. Rosen, M. P. Matheu, M. G. Sanna, S. K. Wang, E. Jo, C. H. Wong, I. Parker, and M. D. Cahalan. 2005. Sphingosine 1-phosphate type 1 receptor agonism inhibits transendothelial migration of medullary T cells to lymphatic sinuses. *Nat. Immunol.* 6: 1228–1235.